Biochimica et Biophysica Acta, 681 (1982) 177–190
Elsevier Biomedical Press

BBA 41118

A METHOD FOR IN SITU CHARACTERIZATION OF *b*- AND *c*-TYPE CYTOCHROMES IN *ESCHERICHIA COLI* AND IN COMPLEX III FROM BEEF HEART MITOCHONDRIA BY COMBINED SPECTRUM DECONVOLUTION AND POTENTIOMETRIC ANALYSIS

J.E. VAN WIELINK, L.F. OLTMANN, F.J. LEEUWERIK, J.A. DE HOLLANDER and A.H. STOUTHAMER

Department of Microbiology, Biological Laboratory, Vrije Universiteit, De Boelelaan 1087, 1007 MC Amsterdam (The Netherlands)

(Received February 4th, 1982)

Key words: Cytochrome b; Spectrum deconvolution; Potentiometry; (E. coli, Bovine heart mitochondria)

An analytical technique for the in situ characterization of *b*- and *c*-type cytochromes has been developed. From evaluation of the results of potentiometric measurements and spectrum deconvolutions, it was concluded that an integrated best-fit analysis of potentiometric and spectral data gave the most reliable results. In the total cytochrome *b* content of cytoplasmic membranes from aerobically grown *Escherichia coli*, four major components are distinguished with α-band maxima at 77 K of 555.7, 556.7, 558.6 and 563.5 nm, and midpoint potentials at pH 7.0 of 46, 174, −75 and 187 mV, respectively. In addition, two very small contributions to the α-band spectrum at 547.0 and 560.2 nm, with midpoint potentials of 71 and 169 mV, respectively, have been distinguished. On the basis of their spectral properties they should be designated as a cytochrome *c* and a cytochrome *b*, respectively. In Complex III, isolated from beef heart mitochondria, five cytochromes are distinguished: cytochrome c_1 (λ_m(25°C) = 553.5 nm; E_0' = 238 mV) and four cytochromes *b* (λ_m(25°C) = 558.6, 561.2, 562.1, 566.1 nm and E_0' = −83, 26, 85, −60 mV).

Introduction

Cytochromes *b* and *c* in bacterial and mitochondrial respiratory chains have been characterized either in an isolated and purified state, or in situ in complete systems or functionally substantial parts of respiratory systems such as Complex III in mitochondria (see Refs. 1–3). Especially in connection with the study of specific functions of distinct cytochromes in electron-transport routes, in situ studies are the most important. The cytochromes should be distinguished and recognized by their potentiometric and spectral characteristics in their functional environment. In situ studies avoid the risk of altered physicochemical properties which may occur upon complete solubilization of cytochromes from their specific membranous surroundings (see Ref. 4). Based on the work of Caswell and Pressman [5,6], Wilson and Dutton [7,8] developed a redox titration method for potentiometric characterization of mitochondrial cytochromes. This technique is also often used for the characterization of bacterial cytochromes, unfortunately sometimes with contradictory results (see Refs. 9–17). The resolution of the potentiometric titration method seems to be insufficient for complex, branched bacterial respiratory chains.

For the study of spectral properties of cytochromes, low-temperature (77 K) optical spectra are

Abbreviation: Hepes, 4-(-2-hydroxyethyl)-1-piperazineethanesulphonic acid

often used for better resolution in the composite absorption peaks. Computer-bound spectrum deconvolution, quite generally employed in analytical chemistry (see Refs. 18 and 19), and also in analyses of chlorophyll spectra (see Refs. 20–23), has hardly been used in analyses of cytochrome spectra. Butler and Hopkins [24] and Shipp [25] introduced in this field a peak-finding procedure based on the fourth-order finite difference spectra originally described by Morrey [26]. However, this method might be indicative, but cannot be conclusive about the cytochrome composition of complex systems. As we will demonstrate in this paper, also a spectrum deconvolution (decomposition) method on the basis of best-fit analyses with simulated composite spectra is usually insufficiently reliable for obtaining conclusive evidence on this point. The integration of potentiometric analysis and spectrum deconvolution to one best-fit analysis will bring about the better resolution necessary for the distinction of the various cytochromes *b* and *c* in *Escherichia coli* membranes or in mitochondrial Complex III. These cytochromes will be characterized by their midpoint potentials and their spectral properties as well.

Materials and Methods

Materials. *E. coli* was grown at 37°C in a 14 l fermentor (Microferm, New Brunswick Scientific, Inc., Co.) in 5 l liquid medium containing 0.8% (w/v) Nutrient broth (Oxoid No. 2), 0.5% (w/v) yeast extract (powder, Oxoid No. 21), 0.5% (w/v) glucose and 0.5% (w/v) NaCl. During growth, 10 l air/min was passed through the culture, which was stirred vigorously. Anti-foam (Serva No. 35109) was added when necessary.

Cells were harvested by centrifugation at 15000 $\times g$ for 20 min at 4°C when the culture reached a density of about 0.5 g cells per 1 (dry weight), just before a perceptible production of acid started. The cell paste was washed once in a cold solution of 25 mM Tris-HCl, pH 7.2. After centrifugation at 15000 $\times g$ for 20 min at 4°C, the cells were resuspended in a solution containing 100 mM Hepes, 15 mM $MgCl_2$ and 8 mM EDTA, pH 7.0 (approx. 5 g wet wt./25 ml solution), and broken by passage through a French pressure cell (American Instrument Co.) at 14000 kPa. From the resulting suspension the cytoplasmic membranes were isolated by the use of discontinuous sucrose gradients (layers of 70, 60 and 30% (w/v) sucrose). After 16 h centrifugation at 75000 $\times g$ and 4°C, the cytoplasmic membranes were collected from the dark-coloured layer on the 60% (w/v) sucrose layer by centrifugation (after dilution) at 180000 $\times g$ at 4°C for 2 h. The membranes were resuspended in a solution of 100 mM Hepes, 15 mM $MgCl_2$ and 8 mM EDTA, pH 7.0 (approx. 1 g wet wt./ml solution) and stored at −80°C.

Purified beef heart QH_2 : cytochrome *c* oxidoreductase (Complex III) was a gift from Dr. Simon de Vries (B.C.P. Jansen Institute, University of Amsterdam) and was prepared according the procedure of Hatefi et al. [27], as described elsewhere [28].

Chemicals. The chemicals used were: diaminodurene, 1,2-naphthoquinone, 2-hydroxyl-1,4-naphthoquinone and riboflavin 5′-monophosphate (Fluka AG); phenazine methosulphate (Sigma, St. Louis, U.S.A.); phenazine ethosulphate and trimethylhydroquinone (ICN Pharmaceuticals, Plainview, NY); 2-methyl-1,4-naphthoquinone (menaphthone, vitamin k_3) (Koch-Light Laboratories Ltd., Coinbrook, U.K.); benzyl viologen (British Drug Houses Ltd., Poole, U.K.). Argon N60 ($O_2 \leq 0.1$ ppm) was obtained from Aga Gas B.V. (Amsterdam). All other chemicals were from Merck (Darmstadt, F.R.G.).

Equipment and procedures. Potentiometric titrations were essentially done as reviewed by Wilson [29] and Dutton [30]. They were performed in a DW-2a™ spectrophotometer (American Instrument Co.) equipped with a magnetic stirrer accessory. The 3 ml glass cuvette, in which the titrations were performed, was fitted with a Teflon stopper with gaps for a platinum electrode, an Ag/AgCl reference electrode, an argon gas line and a gap for degassing and additions by means of 10-μl syringes. The dimensions of the platinum electrode were 1 × 5 × 20 mm. It was sandpapered and flamed after each titration to maintain a fast response. The Ag/AgCl electrode was made according to the description of Wilson [29]. Before and after each potentiometric titration, the electrode combination was calibrated by measuring the potential of a saturated solution of quinhydrone in 50 mM potassium hydrogen phthalate at 25°C.

Potentials were measured with a Philips digital pH/mV-meter PW 9408.

For a fast exchange between electron carriers in the membranes and the platinum electrode, and also to stabilize the potentials, titration was carried out in the presence of: 0.4 mM diaminodurene ($E_0' = +275$ mV); 0.1 mM trimethylhydroquinone ($E_0' = +115$ mV); 0.1 mM phenazine methosulphate ($E_0' = +85$ mV); 0.1 mM phenazine ethosulphate ($E_0' = +65$ mV); 0.4 mM 2-methyl-1,4-naphthoquinone ($E_0' = +10$ mV); 1.2 mM tetramethyl-*p*-benzoquinone ($E_0' = +5$ mV); 12.5 μM 2-hydroxy-1,4-naphthoquinone ($E_0' = -145$ mV); 12.5 μM riboflavin 5'-monophosphate ($E_0' = -219$ mV); 12.5 μM anthraquinone-2-sulphonate ($E_0' = -225$ mV) and 1 μM benzyl viologen ($E_0' = -350$ mV). O_2 was excluded from the cuvette by flushing continuously with ultrapure argon ($O_2 \leq 0.1$ ppm) supplied through a stainless-steel pipe-line. Reductive titrations were performed by stepwise addition of anaerobic solutions of NADH or, at lower oxidation potentials, dithionite. In oxidative titrations (always started with a fresh sample), at first the redox carriers were reduced by the addition of NADH and dithionite, before they were stepwise oxidized by the addition of an anaerobic solution of ferricyanide. Concentrations of reduced cytochromes *b* and *c* were correlated to peak areas underneath the α-band recorded in the dual-wavelength mode in the range 540–580 nm. The absorbance at 540 nm was used as reference. For measuring facilities such as baseline correction, calculation of peak area, scan averaging, generation of fourth-order difference spectra (according to the method of Savitsky and Golay [31] with the corrected tables of Steiner et al. [32]), etc., the spectrophotometer was on-line and real-time connected to a PDP 11/03 microcomputer (Digital Equipment Co.), equipped with 28K memory and a multichannel 12-bit data acquisition system (Data Translation, DT 1765). For data storage and retrieval the microcomputer was on-line connected to a central disc-based minicomputer facility (Hewlett-Packard, 21 M-E with RTE IV-B). The whole measurement set-up simulated a 9600-baud terminal to the Hewlett-Packard minicomputer.

When the potentiometric titration was coupled to the recording of 77 K spectra, the spectrophotometer was equipped with a low-temperature accessory (J4-9603, American Instrument Co.). The special cuvettes had a capacity of 1.0 ml and a path length of 2 mm. To improve the signal-to-noise ratio, all 77 K spectra used in this work are the average of nine sequential scans. In this experimental set-up the titration was carried out in a 35 ml glass vessel instead of the 3 ml glass cuvette described above. Similarly to the 3 ml cuvette, the 35 ml glass vessel was fitted with electrodes and gaps for the argon gas line and for degassing. Moreover, this system contained a siphon for transfer of samples from the vessel into the argon-flushed cuvette under anaerobic conditions. Immediately after the transfer the samples were frozen in liquid nitrogen. Except for some elbows, made of Teflon tubing, all pipes in the system were made of stainless steel, in order to diminish contamination with O_2. Protein was essayed by the biuret method with bovine serum albumin as standard [33].

Data analysis. For the determination of best-fitting curves to sets of data points on the basis of a given function for the description of these curves, a computer programme was developed which optimizes such a fit by means of non-linear least-squares analysis *. As a numerical criterion of the quality of the fit the value of SS is used, which is defined as the sum of squared differences between experimental and predicted points. Using the gradient-expansion algorithm of Marquardt [34], the programme finds optimum values for the variable parameters in the given function by minimizing SS with respect to each of the parameters simultaneously.

The procedure of Marquardt [34] combines the best features of the gradient search and the analytical search. It implies the use of a gradient search when the solution is far off the final one, whereas an analytical search, in which the function is linearized with respect to its parameters, is used when the solution approaches its optimum. In this way an iterative search is constructed which converges rapidly. The programme is multipurpose, dependent on the chosen function. It was used for

* On request, subroutines written in Fortran IVB are available.

the analysis of potentiometric measurements, spectrum deconvolution and the combination of both.

Results

Potentiometric titrations

Suspensions of cytoplasmic membranes, isolated from aerobically grown *E. coli*, were submitted to potentiometric titrations in order to characterize the membrane-bound cytochromes *b* and *c*. A typical set of resulting data points is presented in Fig. 1. These data points should fit to a curve which has to be constructed on the basis of the Nernst equation. Therefore, the Nernst equation should be transposed into a form which describes the area (AR) of the composite α-band of cytochromes *b* and *c* as the sum of partial contributions of *n* components with different midpoint potentials ($E'_{0,i}$) as they depend on the oxidation-reduction potential (E) of the suspension. In the formula:

$$AR(E) = \sum_{i=1}^{n} AR_i^* \left[1 + \exp\{(E - E'_{0,i})/25.68\}\right]^{-1}$$

each component is thus characterized by two parameters; AR_i^*, the area underneath the α-band of component i at full reduction and $E'_{0,i}$, the midpoint potential at pH 7.0 of component i. For the interpretation of titration results, one has to estimate those values of AR_i^* and $E'_{0,i}$, which yield, for a given number of components (n), the best fit of the curve to the experimental data. Such a non-linear least-squares analysis can easily be done by a computer programme, which calculates optimal parameter values minimizing an SS value defined as the sum of squared differences between experimental and predicted points (see Material and Methods). Unfortunately, one cannot find an objective criterion for the number of components in the titration results, which turned out to be one of the greatest difficulties in potentiometric titration assays on cytochromes in situ. The more parameters are taken into account, the better will be the fit of the curve, up to a statistically defined maximum value of n, beyond which the resolution of the data set fails and the fit will not be improved any more.

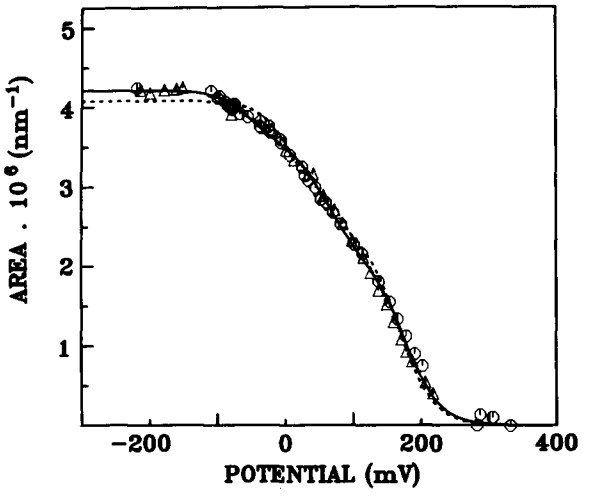

Fig. 1. Potentiometric titration of cytochromes *b* and *c* in cytoplasmic membranes from aerobically grown *E. coli*. Peak areas of α-bands in the 540–580 nm range are plotted vs. the redox potential. The redox potential was varied by the addition of NADH or dithionite (△) and ferricyanide (○). The dashed line and the solid line represent best-fit analyses for two and three components, respectively. The protein concentration was 15 mg/ml.

In Table I, we present sets of best-fitting parameter values for various numbers of cytochromes supposed to contribute to the α-band between 540 and 575 nm. Obviously, the resolution allows at most the distinction of four components, since the value of SS does not decrease any further beyond that number of components. From Fig. 1 it is clear that the two-component fit is rather inferior. A choice between the three- and four-component fit is hardly possible. It is remarkable, and rather typical of titration analyses, that the values of midpoint potentials and proportional contributions of components, which are distinguished, seriously differ depending on the number of components (Table I).

One should conclude that the resolution of the potentiometric titration method is insufficient to be conclusive about the characteristics of cytochromes in *E. coli* membranes.

Spectrum deconvolution

In an attempt to complete the results of potentiometric titrations, we developed a method for deconvolution of the α-band between 540 and 575 nm at 77 K in absolute optical spectra of dithionite-reduced cytoplasmic membranes from aerobically grown *E. coli*.

TABLE I

SETS OF BEST-FITTING PARAMETERS FOR THE POTENTIOMETRIC TITRATION OF CYTOCHROMES *b* AND *c* IN CYTOPLASMIC MEMBRANES FROM AEROBICALLY GROWN *E. COLI*

The percentage expresses the proportional contribution of a component to the fully reduced optical absorbance band between 540 and 575 nm. E_0' expresses the midpoint potential at pH 7.0 of the concerning compound. SS (in arbitrary units) represents the sum of squared differences between experimental and predicted points.

%	E_0'	%	E_0'	%	E_0'	%	E_0'	%	E_0'	%	E_0'
10	−80	10	−80	11	−76						
						16	−54				
5	16										
		21	15	25	27			37	18		
16	16					33	61				
18	88	18	87								
				30	122					87	130
33	157	33	157								
						50	176	59	166		
18	211	18	211	33	194						
SS=87		SS=87		SS=90		SS=143		SS=433		SS=6133	

Two presuppositions were made. Firstly, we assumed that the shape of optical bands as measured with a spectrophotometer can be described reasonably by Gaussian functions, which are symmetrical on the energy scale. Secondly, we considered the baseline in our spectra of fully reduced samples to be a straight line. Light scattering did not cause serious deviation between 540 and 580 nm.

According to these presuppositions, the absorbance (A) as a function of the wavelength (λ) in a composite α-band can be described as the sum of n Gaussians (symmetric on the wave number scale) in the formula:

$$A(\lambda)=\sum_{i=1}^{n} A_{m,i}\cdot\exp\left\{-4\ln 2\cdot\lambda_{m,i}^2(\lambda_{m,i}-\lambda)^2/\lambda^2 w_{\lambda,i}^2\right\}$$

where $A_{m,i}$ is the absorbance maximum of component i, $\lambda_{m,i}$ the wavelength at the absorbance maximum of component i and $w_{\lambda,i}$ the bandwidth on the wavelength scale of component i at $A = 1/2A_{m,i}$.

Each of the components is now characterized by three parameters, viz., $A_{m,i}$, $\lambda_{m,i}$ and $w_{\lambda,i}$. Just as described in the previous section for the interpretation of potentiometric titrations, the best-fitting values of these parameters can be calculated by a similar computer non-linear least-squares analysis. Again, an objective basis for selection of the right number of components is lacking. In

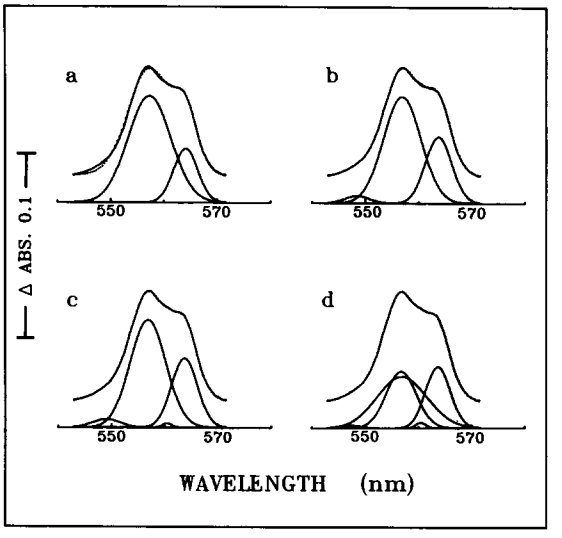

Fig. 2. Decomposition of a cytochrome *b*/*c* α-band of dithionite-reduced cytoplasmic membranes from aerobically grown *E. coli*. The spectrum (upper solid line in each panel), recorded as an averaged absolute spectrum at 77 K with the absorbance at 540 nm as reference, is decomposed into two (a), three (b), four (c) or five (d) components (solid lines on the abscissa). The dotted lines (only perceptible in traces a and b) represent the predicted spectrum as the sum of composing Gaussians. The protein concentration was 15 mg/ml.

TABLE II

SETS OF BEST-FITTING PARAMETERS FOR THE α-BAND OF CYTOCHROMES *b* and *c* IN DITHIONITE-REDUCED CYTOPLASMIC MEMBRANES FROM AEROBICALLY GROWN *E. COLI*

The percentage expresses the proportional contribution of a component to the optical absorbance band, λ_m represents the wavelength of its absorbance maximum and *w* is the bandwidth at half-height. SS (in arbitrary units) represents the sum of squared differences between experimental and predicted points.

%	λ_m	*w*	%	λ_m	*w*	%	λ_m	*w*	%	λ_m	*w*	%	λ_m	*w*	%	λ_m	*w*
2	548.5	5.5	1	547.5	4.1				3	548.4	5.5						
						5	549.5	6.6									
5	553.5	4.2										77	557.1	9.4			
22	556.9	5.2	28	556.8	6.7	59	556.6	7.5	67	556.8	8.2						
42	557.0	10.8	45	557.0	11.0												
															102	558.7	12.3
2	560.3	2.8	1	560.4	2.2												
						34	563.2	6.4	30	563.7	5.8	22	564.0	5.3			
28	563.6	5.6	25	563.7	5.5												
						2	564.6	3.0									
SS = 44			SS = 51			SS = 79			SS = 130			SS = 1153			SS = 16607		

Fig. 2 the results of the decomposition into two, three, four and five components are depicted. The associated parameter values, up to a six-component decomposition, are given in Table II.

As can be seen in Fig. 2, the fit with less than three components is unsatisfactory. With three or more components the curve simulation fits very well with the original spectrum. Beyond four components an improvement in the fit is barely visible. The visual judgement of the fit can be improved considerable by making use of fourth-order finite difference curves, which can be generated from the original spectrum and the simulated curve as well. The technique of fourth-order difference spectra, based on an idea of Morrey [26], was introduced by Butler and Hopkins [35] for the analysis of complex chloroplast spectra. Later on this technique was used by Shipp [36] and Poole et al. [37] as a method for decomposition of cytochrome spectra. We applied this method on simulated composite spectra, which were constructed in agreement with our final solution for the cytochrome composition in aerobically grown *E. coli* (see below). The fourth-order finite difference curve, as well as the mathematical fourth-derivative spectrum, which can both be constructed in this case, failed in the distinction of all components at the right wavelength (results not shown). Furthermore, quantitation of the components was completely impossible, since the peak heights in fourth-derivative spectra are mainly determined by the bandwidths of components. On the other hand, providing that fourth-order finite different spectra can be generated which are completely free of the influence of noise on the original experimental spectra, it seems a reasonable stipulation that the fourth-order difference curve from the composite spectrum and the one from the spectrum simulation should be similar. In Fig. 3 the fourth-order difference curves are added to the decomposition results. Obviously, at least five components are needed for a reasonable fit of the two fourth-order difference curves.

In Table II, it can be concluded from the SS values that the quality of the fit is scarcely improved by the introduction of more than five components. So far, the five-component fit seems to be a reasonable choice as a final solution. However, on comparing parameter values in the

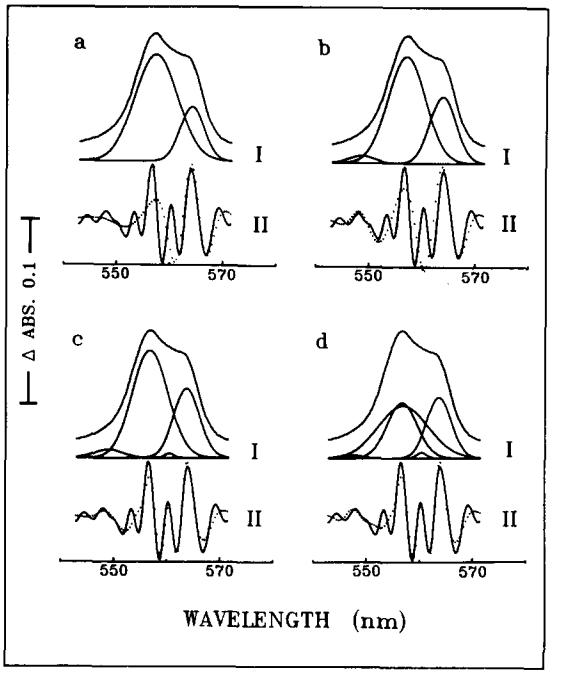

Fig. 3. Spectrum decomposition and fourth-order finite difference curves. The curves designated by I represent the same spectrum decomposition as illustrated in Fig. 2. The curves designated by II represent the fourth-order finite difference curves generated from the original spectrum (solid lines) and from the predicted spectrum (broken lines).

solutions for different numbers of components, it is noteworthy that they are rather variable. The very wide major component at 557.0 nm in the five-component solution is not recognizable in the four-component fit. It appears to be questionable whether all components which are introduced in the spectrum deconvolution represent definite cytochromes or merely fill up the peak area in the spectrum as a result of possible casual or systematic differences between the original band shape and the chosen function for spectrum simulation.

Integration of potentiometric titration in spectrum deconvolution

For a better guarantee of the physical reality of components which are introduced during spectrum deconvolution, we added an additional criterion to the deconvolution procedure: Each component which fits in a spectrum should also satisfy the

Nernst equation, taking into consideration series of spectra recorded with one preparation at various oxidation-reduction potentials. In other words, it means that the described potentiometric titration procedure is integrated into the spectral decomposition procedure. In the formula, the absorbance (A) in composite α-bands, as a function of wavelength (λ) and oxidation-reduction potential (E), should be described by:

$$A(\lambda, E) = \sum_{i=1}^{n} A^*_{m,i}\left[1+\exp\{(E-E'_{0,i})/25.68\}\right]^{-1} \cdot \exp\left\{-4\ln 2 \cdot \lambda^2_{m,i}(\lambda_{m,i}-\lambda)^2/\lambda^2 w^2_{\lambda,i}\right\}$$

where $A^*_{m,i}$ is the absorbance maximum of component i at full reduction, $E'_{0,i}$ the midpoint potential of component i at pH 7.0, $\lambda_{m,i}$ the wavelength at the absorbance maximum of component i, $w_{\lambda,i}$ the band width on the wavelength scale of component i at $A = 1/2A_{m,i}$ and n the number of components.

Now, the computer analysis has to optimize, for a given number of components, four parameters per component, viz., $A^*_{m,i}$, $\lambda_{m,i}$, $w_{\lambda,i}$ and $E'_{0,i}$. The integration of both potentiometric analysis and spectrum deconvolution has a number of advantages over the separate application of both methods: better resolution, since many more

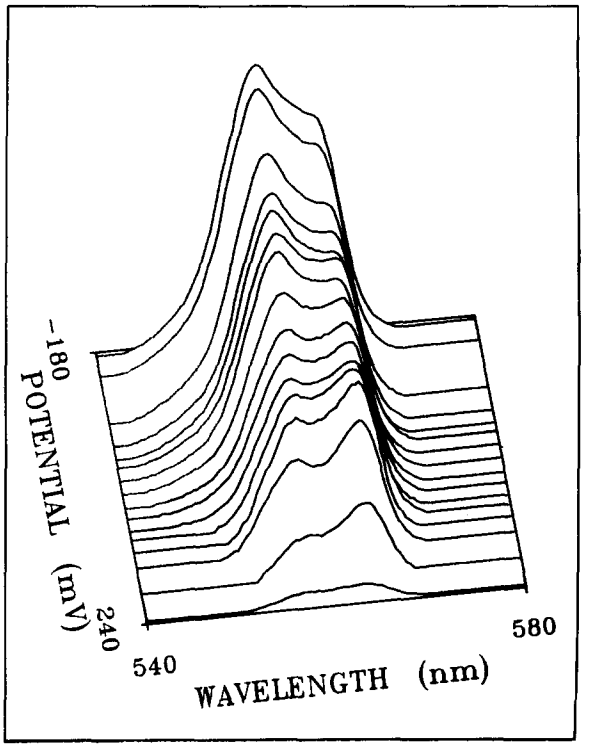

Fig. 4. Three-dimensional plot of 77 K spectra of cytoplasmic membranes from aerobically grown *E. coli*, taken at different redox potentials. The absorbance is plotted perpendicular to the plane determined by the wavelength and potential axes. The protein concentration was 15 mg/ml.

TABLE III

SETS OF BEST-FITTING PARAMETERS FOR CYTOCHROMES *b* AND *c* IN CYTOPLASMIC MEMBRANES ISOLATED FROM AEROBICALLY GROWN *E. COLI*

The analyses refer to a series of 16 α-band cytochrome spectra, recorded at redox potentials ranging between −174 and 236 mV. The samples were frozen at 77 K during scans of the spectra. The percentage expresses the proportional contribution of a component to the total area of the α-band at full reduction, λ_m represents the wavelength of its absorbance maximum, w is the bandwidth at half-height and E'_0 represents the midpoint potential at pH 7.0. SS (in arbitrary units) represents the sum of squared differences between experimental and predicted points.

%	λ_m	w	E'_0	%	λ_m	w	E'_0	%	λ_m	w	E'_0	%	λ_m
9	550.3	7.7	56	1	547.0	4.6	71						
6	553.7	4.2	49										
				34	555.7	10.3	46	36	555.5	11.3	48	36	555.6
2	556.1	2.6	21										
29	557.2	7.3	173	26	556.7	6.8	174	25	556.6	6.5	174	27	556.8
12	558.5	11.4	−79	13	558.6	11.0	−75	13	558.3	10.0	−70	13	558.3
19	558.5	8.1	43	1	560.2	2.3	169	1	560.1	2.5	170		
23	563.7	5.5	189	24	563.5	5.5	187	25	563.5	5.6	189	25	563.4
SS=30				SS=32				SS=36				SS=43	

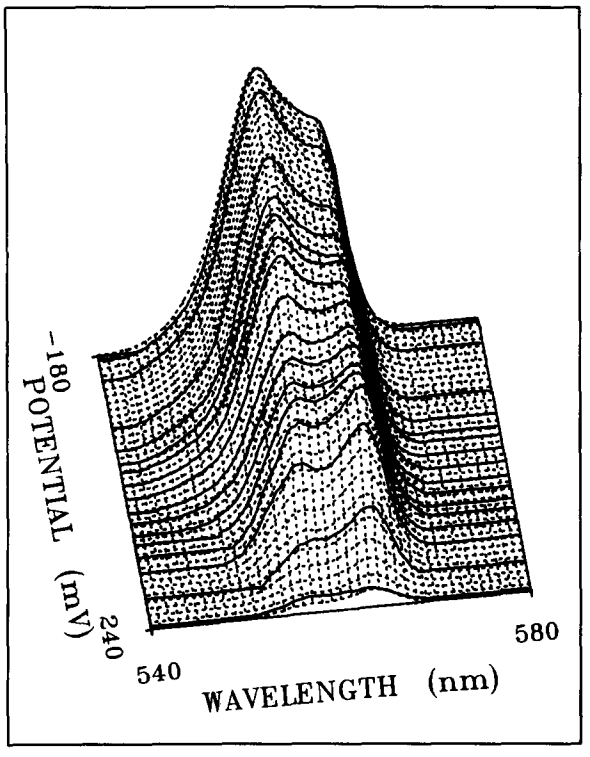

Fig. 5. Combined analysis of potentiometric and spectral data. The solid lines represent the same *E. coli* spectra as drawn, in a similar way, in Fig. 4. The reticular broken lines represent the best-fitting six-component solution (see Table III).

experimental data can be taken into account (decades of spectra recorded at different potentials); spectral properties and midpoint potentials of cytochromes which can be distinguished are unambiguously coupled; more certainty about the reality of introduced components, since they are now independent of possible casual or systematic aberrations in one spectrum.

The integrated fit procedure was applied to a series of 16 α-band cytochrome spectra of cytoplasmic membranes isolated from aerobically grown *E. coli*. These spectra were recorded at 77 K, and spanned a redox-potential range between -174 and $+236$ mV. Since the optical path length of frozen samples may be variable, all 77 K spectra were normalized by multiplication according to the ratio of their total peak areas at 77 K and the total peak area measured with the same preparation under the same redox potential at 25°C. In Fig. 4 the set of spectra is given in a three-dimensional plot ranged according to the redox potentials at which they were recorded. In Fig. 5 the spectra are drawn in a similar way, but in this figure the computer fit, based on a six-component solution, is also added. In Table III parameter values for this solution and others are given.

Evaluating these solutions from $n = 1$ to the most complex solution in Table III ($n = 7$), it is obvious that at first four major components were

half-height and E_0' represents the midpoint potential at pH 7.0. SS (in arbitrary units) represents the sum of squared differences between experimental and predicted points.

w	E_0'	%	λ	w	E_0'	%	λ	w	E_0'	%	λ	w	E_0'
11.2	47	43	556.0	11.6	25	66	556.2	8.3	100				
6.8	174	32	556.8	7.2	167								
9.9	−71									100	558.9	12.4	132
5.8	189	25	563.5	5.7	190	33	563.2	6.5	192				
		SS=95				SS=808				SS=2815			

introduced, while in the $n = 5$ and $n = 6$ solution only two additional minor components appeared. With a seventh set of parameters, the solution of the fit seemed to degenerate. Without a substantial improvement of the fit (see SS values), the broad spectral band at 555.7 nm appeared to be split up into three components with almost equal midpoint potentials around 46 mV. In the latter solution the minor component at 547.0 nm was ignored, however, in the eigth-component fit (not shown) this minor component was reintroduced.

It should be concluded that the six-component solution in Table III is the most realistic one. It means that in the spectrum of aerobically grown *E. coli* membranes, four major α-bands of cytochromes *b* are distinguished at 555.7, 556.7, 558.6 and 563.5 nm, related to midpoint potentials of 47, 174, −71 and 189 mV, respectively. Whether the two bands at 556.7 and 563.5 nm, which have almost similar midpoint potentials, should be attributed to two different cytochromes *b* or to one cytochrome *b* with a double α-band cannot be decided at the moment. The minor peak at 560.2 nm ($E_0' = 169$ mV), which has a very small bandwidth, might also be considered as an extra optical phenomenon of the latter *b*-type cytochrome. Nota bene in the fit of the fourth-order difference spectrum, the presence of this peak with small bandwidth is highly significant (cf. Fig. 3b and c; see

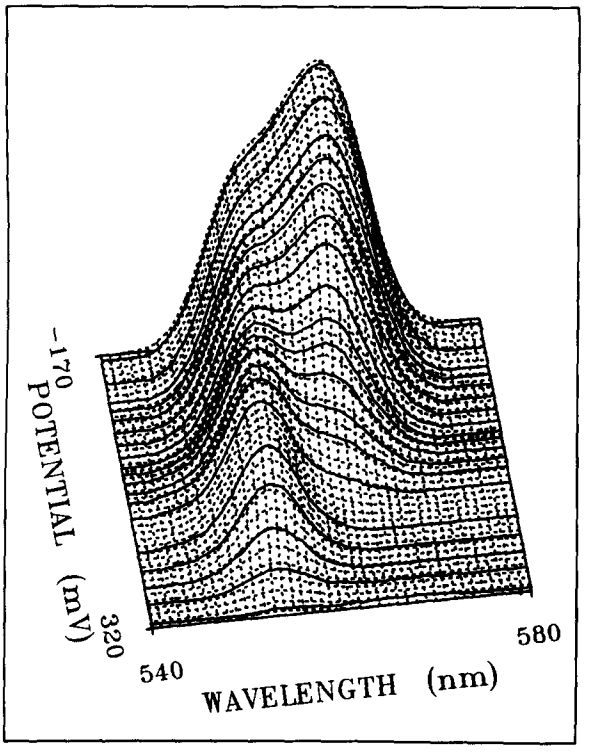

Fig. 6. Combined analysis of Complex III spectra. A set of 19 absolute spectra (solid lines), recorded with purified Complex III at 25°C and at different redox potentials, is plotted in a three-dimensional way as described in the legend to Fig. 4. The best-fitting six-component solution (see Table IV) is presented by the reticular broken lines. The absorbance at full reduction in the peak maximum at 563 nm was 0.055. The protein concentration was 0.22 mg/ml.

TABLE IV

SETS OF BEST-FITTING PARAMETERS FOR CYTOCHROMES *b* AND *c* IN COMPLEX III FROM BOVINE HEART

The analyses refer to a series of 19 spectra, recorded between 540 and 580 nm, at 25°C and redox potentials ranging from −161 to 313 mV. The percentage expresses the proportional contribution of a component to the total area of the α-band at full reduction, λ_m represents the wavelength of its absorbance maximum, *w* is the bandwidth at half-height, and E_0' represents the midpoint potential at pH 7.0. SS (in arbitrary units) represents the sum of squared differences between experimental and predicted points.

%	λ_m	*w*	E_0'	%	λ_m	*w*	E_0'	%	λ_m	*w*	E_0'	%	λ_m
2	552.4	5.2	81	3	553.0	6.0	86	4	553.6	6.6	63		
												22	553.5
14	553.2	8.2	239										
				21	553.6	7.9	242	21	553.5	7.8	242		
7	554.2	6.8	248										
8	557.8	7.8	17	17	560.0	9.6	20						
13	558.5	9.9	−79	12	558.1	9.6	−78	13	557.9	9.0	−75	14	558.6
18	561.5	8.3	86	18	561.7	8.1	85	17	561.7	8.4	88	17	562.1
21	563.7	8.7	22	12	565.0	8.0	19	28	562.4	9.9	24	29	561.2
17	566.4	9.8	−69	18	566.2	8.0	−70	18	566.2	7.6	−68	18	566.1
SS=24				SS=25				SS=28				SS=45	

also Table II), which, in contrast, clearly demonstrates the shortcomings of quantitative analyses based on those fourth-order difference spectra.

The introduction of a minor peak at 547.0 nm, referring to a midpoint potential of 71 mV, did not lead to a significant reduction of SS (see Table III), but the presence of this component, which should be ascribed to a cytochrome *c* on the basis of the wavelength of its absorbance maximum (see Ref. 1), seemed to be significant in the visual judgement of plots like that presented in Fig. 5.

For extra verification of the integrated fit procedure, we also applied it to a very well documented system, namely QH_2: cytochrome *c* oxidoreductase (Complex III), isolated from beef heart mitochondria. A series of 19 spectra was taken between 540 and 580 nm at 25°C in the redox-potential range between −161 and +313 mV. Spectra and the six-component simulation are drawn in Fig. 6; the best-fitting values of the parameters are given in Table IV.

The four-component fit, with peaks at 553.5 nm (cytochrome c_1) and 557.5, 561.9 and 565.8 nm (cytochromes *b*) with midpoint potentials of 237, −55, 60 and −56 mV, respectively, is in good agreement with previously published values in the literature (see Ref. 3). Introduction of one more component led to splitting up of the 561.9 nm band into two bands with different midpoint potentials at 26 and 85 mV. Apart from a deviation in the latter midpoint potential, this result confirms the previously described inhomogeneity of the 562 nm band by Berden et al. [38]. Furthermore, the splitting of this band is supported by EPR studies on Complex III [28].

In view of the SS value, the quality of the fit is further improved by the introduction of a sixth minor component at 553.6 nm and a midpoint potential of 63 mV. The relevance of this peak is unclear at the moment. Beyond six components, the solutions again exhibited degeneration. The final conclusion should be that the five- and six-component solution is the most realistic one, leaving aside the meaning of the small extra band at 553.6 nm.

Discussion

In the literature, several rather conflicting results of potentiometric titrations of cytochromes *b* and *c* in *E. coli* cytoplasmic membranes can be found [10–15]. The principal reason for these discrepancies seems to be the insufficiency of the resolution of commonly used titration methods for the analysis of complex respiratory chains. Also, the resolution, and the reliability of spectrum analyses on the basis of fourth-order finite difference curves [26,36,37] are insufficient for this purpose. The shortcomings of both methods are clearly demonstrated in Results. The new method

represents the wavelength of its absorbance maximum, *w* is the bandwidth at half-height, and E_0' represents the midpoint potential at pH 7.0. SS (in arbitrary units) represents the sum of squared differences between experimental and predicted points.

w	E_0'	%	λ_m	*w*	E_0'	%	λ_m	*w*	E_0'	%	λ_m	*w*	E_0'
7.7	238	22	553.5	7.7	237	23	553.5	7.7	234	29	553.8	8.3	230
10.8	−83	16	557.5	9.9	−55								
7.9	85												
		38	561.9	9.2	60	39	562.1	9.7	60				
11.5	26									71	562.5	10.4	24
7.4	−60	24	565.8	8.2	−56	38	563.0	12.7	−57				
		SS=89				SS=261				SS=1402			

of integrated potentiometric analysis and spectrum deconvolution, described in this paper, attains the better resolution necessary for analyses of bacterial cytochromes in situ. Moreover, the components are characterized by midpoint potentials as well as by spectral properties. The latter feature is important for further study of the functional aspects of the cytochromes in situ.

In our final results of the analysis of the *E. coli* cytochromes, mutually conflicting data from the literature can be reconciled. Concerning the midpoint potentials, the last values published by Hendler and Shrager [12] (182, 54 and −110 mV) are confirmed for the greater part by our analysis.

The results of Pudek and Bragg [13], who distinguished only two cytochromes with midpoint potentials of 165 and 35 mV, resemble the two-component fit in Table I. However, in our computation, the two-component solution should be rejected as a misinterpretation of the titration results.

The spectral characteristics of the major components which we found agree with the results published by Reid and Ingledew [15], but we disagree with the midpoint potentials which were given to the components by the latter authors.

Two presuppositions had to be made in the combined fit procedure: the Gaussian function, symmetrical on the wave number scale, should describe properly the shape of the α-bands, and the redox properties of the individual cytochromes should fulfil independently the Nernst equation.

In the literature, other functions such as Lorentz functions, Student T3 distributions or mixtures of Lorentz and Gauss functions were used for the description of spectral bands (see Ref. 18, 19, 24, 26 and 39). Being aware that none of these functions describes exactly the bands returned by the spectrophotometer, we selected the Gauss function which turned out to give quite satisfactory results in testing the method on commercially available purified cytochrome *c* from horse heart (results not shown).

In principle, the Nernst equation is only valid in thermodynamically ideal systems. Its application to membrane-bound redox carriers implies some approximation. Moreover, cooperative effects between the haem centres may cause a further deviation, so the midpoint potentials which are measured should be regarded as apparent values. Formerly, there has been discussion in the literature about the influence of energization of the electron-transport particles on the apparent midpoint potentials. Energization effects were not expected in our measurements, since they were always done after the electron transport had come to an end, while a possible membrane potential built up upon the addition of an oxidant/reductant would have been dissipated by that time.

In contrast to least-squares analyses of potentiometric titrations or spectrum deconvolutions performed separately, the solutions found in the combined analyses exhibit constancy in the characteristics of the components which are introduced upon raising the number of parameter sets (see Tables III and IV). Without very serious drift in the estimated spectral and potentiometric characteristics, the major and minor components were introduced one after another. The risk of misinterpretations caused by the choice of a wrong number of components is minimized in that way.

Combining redox and spectral characteristics of distinct cytochromes, the integrated fit procedure is quite suitable for elucidation of the influence of environmental factors in situ upon the redox properties of those cytochromes. Also, the influence of growth conditions on bacterial cytochrome compositions can be analyzed by this method. Such applications will be given in subsequent papers.

Appendix

Derivation of formulae

Nernst equation. Considering the redox reaction, $\text{cytochrome}_{ox} + e^- \rightleftharpoons \text{cytochrome}_{red}$), the Nernst equation describes the relationship between E, the potential with respect to the standard hydrogen electrode, and the ratio $[\text{cytochrome}_{ox}]/[\text{cytochrome}_{red}]$:

$$E = E_0' + RT/F \cdot \ln\{[\text{cytochrome}_{ox}]/[\text{cytochrome}_{red}]\} \quad \text{(A1)}$$

where E_0' ist he midpoint potential of the redox couple at pH 7.0, R the gas constant (0.475 J · degree^{-1} · mol^{-1}), F the Faraday constant (5.508 J · mV^{-1} · mol^{-1}) and T the absolute temperature (K). So at 298 K with E and E_0' in mV:

$$E = E_0' + 25.68 \ln\{[\text{cytochrome}_{ox}]/[\text{cytochrome}_{red}]\} \quad \text{(A2)}$$

or:

$$[\text{cytochrome}_{ox}]/[\text{cytochrome}_{red}]=\exp\{(E-E_0')/25.68\} \quad (A3)$$

Since:

$$[\text{cytochrome}_{ox}]+[\text{cytochrome}_{red}]\approx AR^* \quad (A4)$$

where AR* is the area under the α-band at full reduction and, for the cytochromes *b* and *c* considered here:

$$[\text{cytochrome}_{red}]\approx AR \quad (A5)$$

where AR is the area underneath the α-band, the Nernst equation can be written as:

$$(AR^*-AR)/AR=\exp\{(E-E_0')/25.68\} \quad (A6)$$

or:

$$AR(E)=AR^*[1+\exp\{(E-E_0')/25.68\}]^{-1} \quad (A7)$$

For *n* different *b*/*c*-type cytochromes, AR is the sum of the partial contributions AR_i:

$$AR(E)=\sum_{i=1}^{n} AR_i^*[1+\exp\{(E-E_{0,i}')/25.68\}]^{-1} \quad (A8)$$

where AR_i^* is the area underneath the α-band of component *i* at full reduction, and $E_{0,i}'$ the midpoint potential of component *i* at pH 7.0.

Gauss equation

Here, the Gauss equation is used to describe the absorbance *A* as a function of the wave number *x*:

$$A(x)=A_m\exp\{-4\ln 2(x-x_m)^2/w_x^2\} \quad (A9)$$

where A_m is the absorbance maximum, x_m the wave number at the absorbance maximum, and w_x the bandwidth on the wave number scale at $A=1/2A_m$.

When λ_m is defined as the wavelength at the absorbance maximum and w_λ as the bandwidth on the wavelength scale at $A=1/2A_m$:

$$(x-x_m)^2=(1/\lambda-1/\lambda_m)^2 \quad (A10)$$

or:

$$(x-x_m)^2=(\lambda_m-\lambda)^2/\lambda^2\lambda_m^2 \quad (A11)$$

and:

$$w_\lambda=1/(x_m-w_x/2)-1/(x_m+w_x/2) \quad (A12)$$

or:

$$w_\lambda=w_x/(x_m^2-w_x^2/4) \quad (A13)$$

or:

$$w_\lambda=w_x/x_m^2\ (\text{since } x_m^2\gg w_x^2/4) \quad (A14)$$

or:

$$w_\lambda=w_x\lambda_m^2\ (\text{since } x_m^2=1/\lambda_m^2) \quad (A15)$$

or:

$$w_x=w_\lambda/\lambda_m^2 \quad (A16)$$

From Eqns. A11 and A16 it follows that:

$$(x-x_m)^2/w_x^2=\lambda_m^2(\lambda_m-\lambda)^2/\lambda^2w_\lambda^2 \quad (A17)$$

From Eqns. A9 and A17 it follows that:

$$A(\lambda)=A_m\exp\{-4\ln 2\lambda_m^2(\lambda_m-\lambda)^2/\lambda^2w_\lambda^2\} \quad (A18)$$

A composite α-band can be described as the sum of *n* Gaussians (symmetrical on the wave number scale):

$$A(\lambda)=\sum_{i=1}^{n} A_{m,i}\exp\{-4\ln 2\lambda_{m,i}^2(\lambda_{m,i}-\lambda)^2/\lambda^2w_{\lambda,i}^2\} \quad (A19)$$

where $A_{m,i}$ is the absorbance maximum of component *i*, $\lambda_{m,i}$ the wavelength at the absorbance maximum of component *i* and $w_{\lambda,i}$ the bandwidth on the wavelength scale of component *i* at $A=1/2A_{m,i}$.

Combination of the Nernst equation and the Gauss equation

In Eqn. A7 the area underneath an α-band is written as a function of *E*.

Since:

$$AR(E)=\int_{\lambda=540}^{580} A(\lambda)\,d\lambda \quad (A20)$$

Eqn. A7 can be rewritten as:

$$A_\lambda(E) = A^*_\lambda\left[1+\exp\{(E-E'_0)/25.68\}\right]^{-1} \qquad \text{(A21)}$$

where A_λ is the absorbance at a given wavelength and A^*_λ is equal to A_λ at full reduction.

Combining Eqns. A19 and A21 gives:

$$A(\lambda, E) = \sum_{i=1}^{n} A^*_{m,i}\left[1+\exp\{(E-E'_{0,i})/25.68\}\right]^{-1} \cdot \exp\left\{-4\ln 2\lambda^2_{m,i}(\lambda_{m,i}-\lambda)^2/\lambda^2 w^2_{\lambda,i}\right\} \qquad \text{(A22)}$$

where $A^*_{m,i}$ is the absorbance maximum of component i at full reduction, $E'_{0,i}$ the midpoint potential of component i at pH 7.0, $\lambda_{m,i}$ the wavelength at the absorbance maximum of component i, and $w_{\lambda,i}$ the bandwidth on the wavelength scale of component i at $A = 1/2A^*_{m,i}$.

Acknowledgements

The authors wish to acknowledge the excellent technical assistance of Mr. W.N.M. Reijnders. They are very grateful to Dr. S. de Vries (B.C.P. Jansen Institute, University of Amsterdam) for his gift of purified Complex III and for helpful comments. This investigation was supported by the Netherlands Foundation for Chemical Research (SON), and the Netherlands Foundation for Biological Research (BION), with financial aid from the Netherlands Organization for Advancement of Pure Research (ZWO).

References

1 Haddock, B.A. and Jones, C.W. (1977) Bacteriol. Rev. 41, 47–99
2 Von Jagow, G. and Sebald, W. (1980) Annu. Rev. Biochem. 49, 281–314
3 Rieske, J.S. (1976) Biochim. Biophys. Acta 456, 195–247
4 Yu, C., Yu, L. and King, T.E. (1979) Arch. Biochem. Biophys. 198, 314–322
5 Caswell, A.H. (1968) J. Biol. Chem. 243, 5827–5836
6 Caswell, A.H. and Pressman, B.C. (1968) Arch. Biochem. Biophys. 125, 318–325
7 Wilson, D.F. and Dutton, P.L. (1970) Arch. Biochem. Biophys. 136, 583–585
8 Wilson, D.F. and Dutton, P.L. (1970) Biochem. Biophys. Res. Commun. 39, 59–64
9 Kröger, A. and Innerhofer, A. (1976) Eur. J. Biochem. 69, 497–506
10 Hendler, R.W., Towne, D.W. and Shrager, R.I. (1975) Biochim. Biophys. Acta 376, 42–62
11 Hendler, R.W. (1977) Anal. Chem. 49, 1914–1918
12 Hendler, R.W. and Shrager, R.I. (1979) J. Biol. Chem. 254, 11288–11299
13 Pudek, M.R. and Bragg, P.D. (1976) Arch. Biochem. Biophys. 174, 546–552
14 Reid, G.A. and Ingledew, W.J. (1978) Biochem. Soc. Trans. 6, 1298–1300
15 Reid, G.A. and Ingledew, W.J. (1979) Biochem. J. 182, 465–472
16 Cox, J.C., Ingledew, W.J., Haddock, B.A. and Lawford, H.G. (1978) FEBS Lett. 93, 261–265
17 Willison, J.C., Ingledew, W.J. and Haddock, B.A. (1981) FEMS Microbiol. Lett. 10, 363–368
18 Brouwer, L. and Jansen, J.A.J. (1973) Anal. Chem. 45, 2239–2247
19 Vandeginste, B.G.M. and De Galan, L. (1975) Anal. Chem. 47, 2124–2132
20 French, C.S., Brown, J.S. and Lawrence, M.C. (1972) Plant Physiol. 49, 421–429
21 Leclerc, J.C., Hoarau, J. and Guérin-Dumartrait, E. (1975) Photochem. Photobiol. 22, 41–48
22 Lehoczki, E. (1975) Biochim. Biophys. Acta 408, 223–227
23 Van Ginkel, G. and Kleinen Hammans, J.W. (1980) Photochem. Photobiol. 31, 385–395
24 Butler, W.L. and Hopkins, D.W. (1970) Photochem. Photobiol. 12, 439–450
25 Shipp, W.S. (1971) Biochem. Biophys. Res. Commun. 45, 1437–1443
26 Morrey, J.R. (1968) Anal. Chem. 40, 905–914
27 Hatefi, S., Haavik, A.G. and Jurtshuk, P. (1961) Biochim. Biophys. Acta 52, 106–118
28 De Vries, S., Albracht, S.P.J. and Leeuwerik, F.J. (1979) Biochim. Biophys. Acta 546, 316–333
29 Wilson, G.S. (1978) Methods Enzymol. 54, 396–410
30 Dutton, P.L. (1978) Methods Enzymol. 54, 411–435
31 Savitsky, A. and Golay, J.E. (1964) Anal. Chem. 36, 1627–1639
32 Steiner, J., Termonia, Y. and Deltour, J. (1972) Anal. Chem. 44, 1906–1909
33 Herbert, D., Phipps, P.J. and Strange, R.E. (1971) in Methods in Microbiology (Norris, J.R. and Ribbons, D.W., eds.), Vol. 5B, pp. 244–249, Academic Press. Inc., New York
34 Marquardt, D.W. (1963) J. Soc. Ind. Appl. Math. 11, 431–441
35 Butler, W.L. and Hopkins, D.W. (1970) Photochem. Photobiol. 12, 451-456
36 Shipp, W.S. (1972) Arch. Biochem. Biophys. 150, 482–488
37 Poole, R.K., Scott, R.J. and Chance, B. (1980) Biochim. Biophys. Acta 591, 471–482
38 Berden, J.A., Opperdoes, F.R. and Slater, E.C. (1972) Biochim. Biophys. Acta 256, 594–599
39 Schwartz, L.M. (1971) Anal. Chem. 43, 1336–1338